[CL]

Osmium-isotope ratios of platinum-group minerals associated with ultramafic intrusions: Os-isotopic evolution of the oceanic mantle

Keiko Hattori [a] and Stanley R. Hart [b]

[a] Ottawa-Carleton Geoscience Centre and Department of Geology, University of Ottawa, Ottawa, Ont. K1N 6N5, Canada
[b] Woods Hole Oceanographic Institution, Woods Hole, MA 02543, USA

ABSTRACT

Osmium-isotope ratios were determined by an ion microprobe on the individual platinum-group minerals (PGM) from placers, which are associated with ultramafic intrusions of late Precambrian to Tertiary age. Unlike Os-isotope ratios in large layered mafic intrusions, these $^{187}Os/^{186}Os$ ratios are low, and within a narrow range from 0.99 to 1.12, which is attributed to the occurrences of the intrusions. There was no opportunity to incorporate old crustal Os because of the small sizes of the intrusions and the mode of emplacement into the upper crustal level. In addition, the interaction with the host volcanic rocks of similar age, if any, would not have seriously affected the $^{187}Os/^{86}Os$ ratios of the peridotites.

While different phases of PGM in one grain have similar $^{187}Os/^{186}Os$ ratios, there is a significant variation in a given district. The variation is attributed to a long-term heterogeneity in Re/Os ratios of the oceanic upper mantle.

The lowest value in each area is lower than the value expected from the evolution of bulk Earth composition. The lowering may be due to primordially low Re/Os ratios in the mantle or preferential removal of Re by partial melting to form the continental crust. The former model is rejected because most chondrites have higher Re/Os ratios than type C1 and the core–mantle separation would not have lowered Re/Os ratios. The low $^{187}Os/^{186}Os$ ratios are, therefore, attributed to the extraction of continental crust by preferential removal of Re from the mantle through partial melting. The model is consistent with the depleted nature of oceanic peridotites (positive ϵ_{Nd}, negative ϵ_{Sr}, and low Re/Os ratios).

Calculations of $^{187}Os/^{186}Os$ ratios of the mantle residue suggest that the observed data are in accordance with a model involving the extraction of $\sim 2\%$ melt by fractional fusion from the mantle of C1 chondritic composition at ~ 2.0 Ga. If the bulk Earth has higher Re/Os ratios, as proposed by Martin [1], then the observed data require much larger degrees of partial melting or older mean age of partial melting at ~ 3.0 Ga.

The variation in Re/Os ratios in each area is ascribed to the various degrees of mixing of the depleted mantle source and more fertile material. This may be due to local heterogeneity in the mantle, "marble-cake" like mantle [2] or replenishment of Re and Os from a more fertile source by sulphide ($+CO_2$) in the mantle. Generally higher $^{187}Os/^{186}Os$ ratios found in this study compared with those from the southern African sub-continental lithosphere [3] may be attributed to the nature of the latter which is more isolated than the oceanic mantle from the rest of the mantle.

The occurrence of S in the mantle may influence Re-Os isotope variations and the behavior of S may decouple the Re-Os system from other lithophile radiogenic isotope systems.

1. Introduction

Osmium is one of the platinum-group elements (PGE) and its concentration in crustal rocks is generally orders of magnitude lower than that in peridotites. Therefore, the contribution of Os from crustal rocks to the bulk Earth, either by recycling or partial melting processes, should not have had significant impact on Os-isotopes in the mantle. This led to the proposal of a uniform mantle reservoir for Re and Os and a single line of evolution for $^{187}Os/^{186}Os$ ratios in the mantle during the Earth's history [4], and to the identification of the type of chondrite accreted to the mantle after mantle–core separation [5]. Since the pioneering work by Allègre and Luck [4], several Os-isotope studies have been carried out on mafic igneous bodies and mantle xenoliths. The results from large layered mafic intrusions show a significant variation in $^{187}Os/^{186}Os$ ratios

within the intrusions due to the contributions of crustal Os: the Stillwater [6,7], Bushveld [4,8] and Freetown Layered Complexes [9]. The wide variations of ^{187}Os/^{186}Os ratios within the individual intrusive bodies, therefore, invoked a problem in evaluating the ^{187}Os/^{186}Os values of the source mantle.

This paper presents ^{187}Os/^{186}Os values of PGM associated with ultramafic intrusions in orogenic belts of late Precambrian to Tertiary age (Fig. 1). Osmium-isotope ratios of the ultramafic bodies are expected to be least affected by sialic crustal processes because of the ensimatic environments of their intrusion, the mode of emplacement in the upper crustal level and their relatively small size. They represent the slices of the depleted upper mantle which were obducted or diapirically intruded to the upper crustal level, or the cumulates of mafic magmas formed in the lower oceanic crusts. In either case, the magmas or the solid intrusions did not have an opportunity to interact with old crustal material.

2. Analytical method

Osmium-isotope ratios were determined on individual PGM, mounted in epoxy by secondary ion mass spectrometry using the MIT-Brown-Harvard Cameca IMF 3f ion microprobe. Operating conditions were essentially the same as those described by Allègre and Luck [4] and Hart and Kinloch [8]. Detailed operating conditions and reproducibilities of the analyses were described by Hattori et al. [9]. The primary O⁻ beam current of 4 to 20 nA was focussed to 10 μm and the positive secondary ions were energy filtering through a +50 to 110 volt window. The peaks of 185, 186, 187, 188, and 189 masses were measured during each analysis to correct for the contribution of ^{187}Re and Os-hydrides, and to calculate the mass fractionation factor. Replicate analysis during the course of the study over a ten-month period shows a reproducibility (2σ) of ±0.6%. The precision of each result therefore was given as ±0.6% or the in-run error, whichever was larger.

3. Geology and sample locations

Most of PGM used in the study came from placers associated with ultramafic intrusions. Exceptions were isoferroplatinum in chromitites from the Nizhni Tagil ultramafic massif, the Ural Mountains, and laurites enclosed in chromites in

Goodnews Bay

Atlin
Cariboo
Tulameen

Choco

Nijni-Tagnii
Omoutenaya
Tetshio
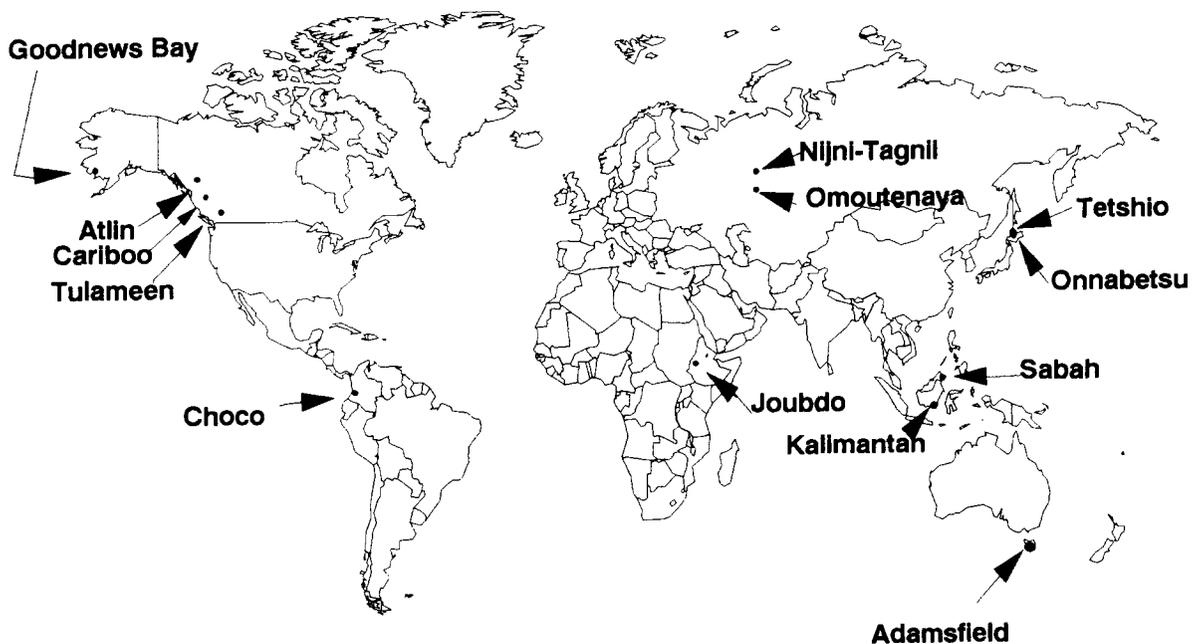Onnabetsu

Joubdo
Kalimantan
Sabah

Adamsfield

Fig. 1. Location map of the samples.

chromitite from the southeastern Kalimantan, Indonesia. Placer occurrences include eluvial (residual) samples, such as PGM from Joubdo, Ethiopia (Fig. 1). The close spatial association of the occurrences of the placers and ultramafic intrusions suggests the derivation of the PGM from the intrusions. The presence of exsolution lamellae in the PGM, which is indicative of high-temperature origin, and common inclusions of pristine olivine and sulphides in PGM confirm the formation of PGM in the intrusion and the mechanical derivation from the ultramafic rocks to the placers [10,11,12].

In this paper, we classify the ultramafic intrusions into non-zoned- and zoned-types to eliminate any confusion arising from common terms such as Alpine-, Alaskan-, Ural-, orogenic-, post-orogenic- and ophiolitic-types. Non-zoned-type intrusions are commonly called "Alpine-type" or "ophiolite-type". They are lenticular in shape and consist of dunite, harzburgite, and lherzolite. A cluster of intrusions commonly form a serpentine belt. The rocks of this type are usually tectonized and partially to completely serpentinized. Non-zoned-type intrusions may be further classified into high and low Ti-groups [13]. The high Ti-group intrusions are believed to be the obducted slices of the depleted upper mantle, while low Ti-group are considered to be the cumulates of high-Mg boninitic magmas [13].

The second classification of intrusions, zoned-type, is commonly called "Alaskan-type", "Ural-type" or "orogenic-type". These intrusions display concentric zoning with a central mass of dunite, surrounded by pyroxenite, and then commonly by gabbro. In some cases, dioritic or syenitic rocks may occur in the outermost rim of the igneous complexes. The intrusions are not highly deformed and primary igneous minerals, such as olivine and pyroxene, are well preserved in most intrusions.

The close spatial association of calc-alkaline volcanic rocks and the chemical compositions of the complexes suggest that the zoned-type ultramafic complexes are related to subduction processes. The origin of the lithological zoning is controversial and proposed opinions include (a) differentiation of ultramafic magmas [14], (b) differentiation of picritic magmas in their feeder pipes [15], or (c) the reaction of later intruded calc-alkaline magma with the pre-existing ultramafic igneous rocks [16]. In models (a) and (b), PGM-bearing chromitites are the early crystallizing phase of the magmas without any crustal contamination. In model (c), the ultramafic bodies of zoned igneous complexes are identical to the non-zoned-type ultramafic intrusions. In any case, the studied samples should represent the Os-isotope values of the oceanic mantle source.

PGM in the non-zoned-type are mostly Os-Ir-Ru minerals such as laurite (RuS_2), erlichmanite (OsS_2), and Os-Ir-Ru metal alloys (hexagonal osmium, ruthenium and rutheniridosmine or cubic iridium). The nomenclature of PGM is after Harris and Cabri [17], in which commonly used "iridosmine" and "osmiridium" are now replaced by hexagonal osmium and cubic iridium or hexagonal rutheniridosmine. Mineral osmium is a phase containing Os as the most abundant PGE. Studied grains are commonly composed of multiple phases of PGM and some PGM show profound chemical zonings, as shown in Cabri and Harris [18].

The PGM within the zoned-type are mainly tulameenite (Pt_2FeCu) and Pt-Fe alloys (cubic isoferroplatinum (Pt_3Fe) or tetragonal tetraferroplatinum (PtFe)) and the PGE are concentrated in chromitites of the dunite cores of the zoned-type complexes. Grains of the Pt-Fe alloy commonly contain crystallographically oriented exsolution lamellae of Ir-Ru-Os alloys and inclusions of laurite/erlichmanite. Osmium-isotope analyses of PGM associated with the zoned-type intrusions were carried out on those Os-bearing inclusions of PGM in the Pt-Fe alloys.

The samples associated with the non-zoned-type intrusions used in this study were from the Cambrian Adamsfield intrusions in Tasmania, the Carboniferous "serpentine belt" in the Cariboo district of southeastern British Columbia, the Pennsylvanian/Permian Atlin intrusions in northwestern British Columbia, the Cretaceous intrusions in Kalimantan, Indonesia, Cretaceous ultramafic belts in the Teshio and Onnabetsu districts of the central Hokkaido Island, Japan, and the Tertiary intrusions in eastern Sabah, Malaysia (Fig. 1). Among them, the Adamsfield intrusions [19] and ultramafic intrusions of the central Hokkaido Island [20] belong to the low Ti-group, defined by Serri [13]. The geology and

occurrences of PGM are described in the Appendix.

The zoned-type samples were from the late Precambrian Joubdo Ultramafic Complex in central western Ethiopia, the southern Ural Mountains in central USSR, the Triassic Goodnews

TABLE 1

$^{187}Os/^{186}Os$ ratios of individual PGM grains

Sample[a]	Phase[b]	$^{187}Os/^{186}Os$[c]	N[d]
NON-ZONED TYPES			
Adamsfield, Tasmania, Australia			
9060862	$Ir_{43}Os_{47}Ru_{10}$ [18]	1.028 ± .006	2
9060863	$Ir_{44}Os_{47}Ru_9$ [18]	1.017 ± .006	5
9060864	$Ir_{66}Os_{27}Ru_7$ [18]	1.013 ± .006	5
9060865	$Ir_{44}Os_{42}Ru_{14}$ [18]	1.014 ± .006	5
9060866	$Ir_{44}Os_{48}Ru_8$ [18]	1.020 ± .006	5
Discovery Creek, Atlin District, Canada			
123391	$Ir_{63}Os_{34}Ru_4$[54]	1.062 ± .006	2
ditto	$Ir_{41}Os_{55}Ru_4$[54]	1.063 ± .006	2
123392	$Ir_{40}Os_{48}Ru_{13}$[54]	1.049 ± .006	2
123395	$Ir_{36}Os_{40}Ru_{24}$[54]	1.063 ± .006	2
123397	$Ir_{70}Os_{28}Pt_3$[54]	1.048 ± .006	3
Atlin, Canada			
10120,1	$Ir_{29}Os_{37}Ru_{34}$[54]		
10120,2	$Ir_{41}Os_{58}Ru_2$[54]	1.050 ± .006	
10120,3	$Ir_{40}Os_{53}Ru_{10}$[54]	1.056 ± .006	2
10120,4	$Ir_{62}Os_{35}Ru_3$[54]	1.047 ± .006	2
10120,9	$Ir_{60}Os_{36}Pt_4$[54]	1.064 ± .006	11
10120,10	iridian osmium	1.039 ± .006	4
10120,11	$Ir_{75}Os_{24}Pt_2$ [54]	1.084 ± .006	3
Ruby Creek, Atline district, Canada			
117352	$Ir_{24}Os_{69}Ru_7$[54]	1.003 ± 006	5
117353	$Ir_{66}Os_{31}Pt_3$[54]	1.016 ± .006	2
117354	$Ir_{17}Os_{81}Ru_2$[54]	1.060 ± .006	2
117355	$Ir_{34}Os_{38}Ru_{28}$[54]	1.030 ± .006	2
117356	$Ir_{37}Os_{30}Ru_{33}$[54]	1.048 ± .006	2
117357	$Ir_{65}Os_{32}Ru_2$[54]	1.049 ± .006	
117358	$Ir_{62}Os_{32}Pt_6$[54]	1.082 ± .006	
Atline district, Canada			
123402	[I]osmian iridium	1.084 ± .006	4
ditto	[M]$Ir_{30}Os_{55}Ru_{15}$[54]	1.047 ± .006	5
ditto	iridium band	1.046 ± .006	3
123403	$Ir_{40}Os_{43}Ru_{17}$[54]	1.054 ± .006	3
123404	$Ir_{42}Os_{56}Ru_3$[54]	1.083 ± .006	3
123405	$Ir_{38}Os_{62}$[54]	1.050 ± .006	6
123406	$Ir_5Os_{93}Ru_2$[54]	1.050 ± .006	2
Bullion deposit, Cariboo district, Canada			
142741	$Ir_{61}Os_{30}Ru_9$[54]	1.030 ± .006	2
	[I]iridian osmium	1.020 ± .006	2
142744	$Ir_{59}Os_{34}Ru_7$[54]	1.039 ± .006	3
Pamali, SE Kalimantan, Indonesia			
26162(L)	laurite	1.039 ± .010	
26163(L)	laurite	1.088 ± .010	
26164(L)	laurite	1.049 ± .007	
Sungai Kalaan, SE Kalimantan, Indonesia			
2636(L)	laurite	1.044 ± .010	
Riam Kanan, SE Kalimantan, Indonesia			
2698	$Pt_6Rh_2Ir_{66}Os_{23}$[55]	1.059 ± .006	4

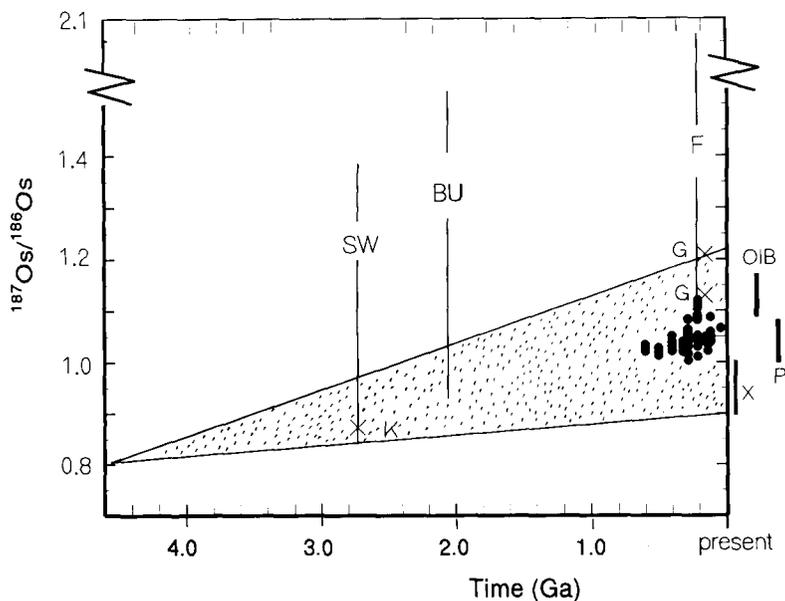| Sample[a]	Phase[b]	$^{187}Os/^{186}Os$[c]	N[d]
Sungai Besar, SE Kalimantan, Indonesia			
31351	$Pt_9Rh_3Ru_3Ir_{51}Os_{31}$[55]		
		1.052 ± .006	5
31352	$Ru_{12}Ir_{40}Os_{44}$[55]	1.052 ± .006	3
3135-3	$Ru_4Ir_{58}Os_{33}$[55]	1.041 ± .006	2
Sungai Edam, SE Sabah, Malaysia			
3092	osmium	1.066 ± .006	3
Teshio, Hokkaido Island, Japan			
01	iridian osmium	1.050 ± .006	6
02	iridian osmium	1.022 ± .006	5
Onnabetsu, Hokkaido Island, Japan.			
01	iridian osmium	1.033 ± .006	4
02	iridian osmium	1.044 ± .006	5
ZONED TYPES			
Joubdo Ultramafic Complex, Birbir district,			
Ethiopia			
24710	[E]osmium(2)	1.022 ± .006	2
	[I]osmium	1.027 ± .006	
24712	[I]osmium	1.027 ± .006	2
24713	[E]osmium	1.023 ± .006	2
	[I]osmium	1.022 ± .006	
24714	[I]osmium(2)	1.029 ± .006	3
Choco, Colombia			
11617A	$Ir_{61}Os_{34}Ru_5$[54]	1.042 ± .006	2
11617B	[I]iridium	1.043 ± .006	3
Bear Creek, Tulameen River, Canada			
124104	$Ir_{87}Os_5Pt_9$[54]	1.049 ± .006	2
	[I]iridium	1.052 ± .007	
Granite Creek, Tulameen River, Canada			
18477	[E]osmium	1.042 ± .008	3
	[I]$Ir_{33}Os_{47}Ru_{19}$[54]	1.011 ± .006	
	[E]$Ir_{36}Os_{55}Ru_9$[54]	1.050 ± .006	2
Lincoln site, Tulameen, Canada			
C-236	[I]laurite	1.083 ± .008	
	[E]osmium	1.087 ± .010	2
	[I]iridian osmium	1.088 ± .006	
Omutnaya River, Sissertj, Ural Mountain, USSR			
U-53	[I]laurite	1.035 ± .010	2
	[I]$Os_{66}Ir_{28}Ru_3Pt_2$[64]	1.037 ± .011	5
Nizhni Tagil, Ural Mountain, USSR			
U-45(L)	[I]rutheniridosmine(2)	1.027 ± .006	2
Goodnews Bay, Alaska			
14NM4	osmium rod	1.119 ± .007	3
	[I]osmium(3)	1.109 ± .007	4
14M4	[E]osmium(2)	1.036 ± .007	2
	[I]osmium(2)	1.043 ± .007	3
GDN1	[I]erlichmanite(3)	1.042 ± .007	4
GDN2	[I]osmium	1.086 ± .007	2
	[E]osmium	1.092 ± .009	2

Fig. 2. $^{187}Os/^{186}Os$ values of PGM associated with ultramafic intrusions, layered intrusions and the mantle-derived rocks. Dots represent the data of PGM in this study. See Fig. 3 for the assigned ages for the plotting of the data. Lines show the range of values observed from layered intrusions: the Bushveld (line BU [4,8]), Stillwater (line SW [6,7]), and Freetown Layered Complexes (line F [9]). Crosses are values of komatiites: cross with K is Archaean komatiite in Abitibi greenstone belt [24]; crosses with G are komatiites from Gorgona Island [50]. Thick lines outside the right y-axis show the ranges of mantle-derived rocks: line with X is xenoliths from South Africa [3]; line with OIB is oceanic island basalts (Hawaii, Iceland [1] and Reunion Island and Loihi [51]; line with P is peridotites [1]. Dotted area indicates possible range of $^{187}Os/^{186}Os$ ratios of the mantle based on 0.805 for the meteorite [52] and the maximum and minimum values observed from the mantle-derived specimens.

Bay Ultramafic Complex on the west coast of Alaska, the Triassic/Cretaceous Choco district in western Colombia, and the Triassic Tulameen Ultramafic Complex in southeastern British Columbia (Fig. 1). The geology and occurrences of PGM in the above areas are found in the Appendix.

4. Results

The Os-isotope ratios of each phase of PGM are listed in Table 1. At least two spots were analyzed for each chemically homogeneous grain. When the grains are heterogeneous in Re, Os and Ir contents, as was common in many cases,

TABLE 2

Range of $^{187}Os/^{186}Os$ ratios of PGM grains in each district

Location	Numbers of phases	Range of $^{187}Os/^{186}Os$
Adamsfield	4	1.013–1.028
Cariboo	3	1.020–1.039
Atlin	24	1.003–1.084
Kalimantan	8	1.039–1.088
Sabah	1	1.066
Teshio	4	1.022–1.050
Onnabetsu	2	1.033–1.044
Joubdo	9	1.022–1.034
Ural Mountains	9	1.021–1.051
Goodnews Bay	13	1.030–1.121
Choco	2	1.042–1.043
Tulameen	9	1.011–1.087

Notes to Table 1:

(a) Numbers followed by (L) are lode samples (collected from the ultramafic rocks).

(b) The nomenclature of PGE alloys are after Harris and Cabri [17]. "Iridosmine" and "osmiridium" are now replaced by osmium and iridium, respectively. The name "rutheniridosmine" is restricted for a hexagonal alloy with Ir as the major element. Numbers in parentheses are numbers of analysed grains. [I] indicates the analyzed phase is a inclusion in isoferroplatinum or tetraferroplatinum. [E] indicates the analyzed phase is an exsolution lamella within isoferroplatinum or tetraferroplatinum.

(c) The precision given in the table is the maximum of individual analyses of the phase. The precision for a single analysis is calculated from the ratio counting statistics or 0.6%, whichever is larger. Further explanation is given in the text.

(d) Number of analyses.

the $^{187}Os/^{186}Os$ ratios of at least four areas were determined on individual grains. Because no variations were found in $^{187}Os/^{186}Os$ ratios within a grain, even in the grains with large chemical variations and zonings, the average values of individual grains are given in Table 1.

Because the Re contents of all samples are low, there is essentially no contribution of radiogenic ^{187}Os to the measured ^{187}Os. Therefore, the measured $^{187}Os/^{186}Os$ ratios are the initial ratios at the time of the formation of PGM. To check Re contents quantitatively, one iridian osmium sample, which showed the highest Re abundance during the ion microprobe analyses (^{187}Re constituting 20% of the mass 187) was examined in the electron microprobe. The ReL_α peak was not detected by counting for 60 s at 20 kV with the beam current 25 nA, which indicates that the

concentration is less than 0.06 wt.%. Thus, the Re/Os weight ratio is less than 0.001. Then, the increase in $^{187}Os/^{186}Os$ due to the in-situ decay of ^{187}Re would be only 0.0003 in a 500 Ma period. The observed values are safely assumed to be the initial values.

The values of $^{187}Os/^{186}Os$ ratios range from 0.992 to 1.121 (Fig. 2). There is no systematic difference in $^{187}Os/^{186}Os$ ratios between PGM from non-zoned- and those from zoned-types. The PGM within a given nugget show similar $^{187}Os/^{186}Os$ ratios within analytical uncertainty independent of the mineral phases. For example, an iridium inclusion in an iridian osmium grain from Discovery Creek in the Atlin district has a $^{187}Os/^{186}Os$ ratio of 1.062, which is similar to the value of the hosting osmium, 1.064 and 1.061 (sample 12339,1; Table 1). Different inclusions of
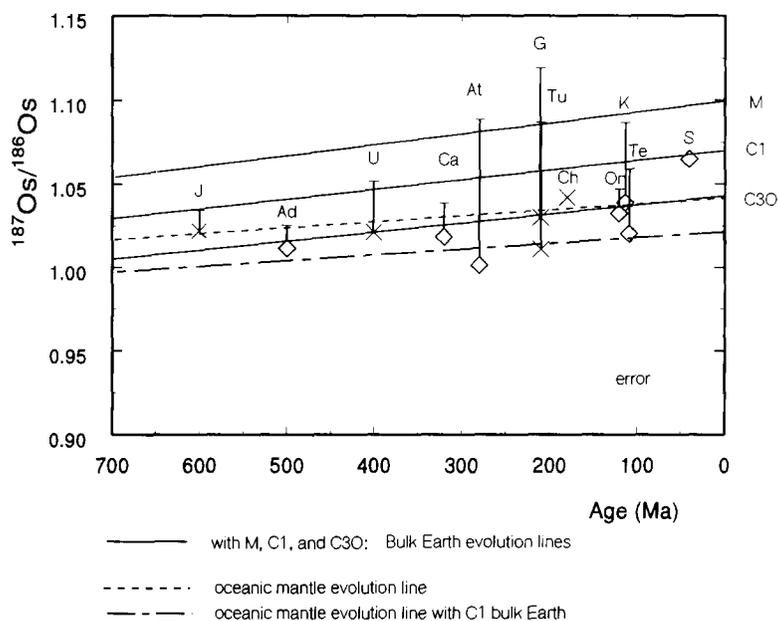

Fig. 3. Minimum values of $^{187}Os/^{186}Os$ for PGM and mantle evolution lines: × = minimum value of $^{187}Os/^{186}Os$ for PGM associated with zoned-type ultramafic intrusions; ◇ = minimum value of $^{187}Os/^{186}Os$ for PGM associated with non-zoned-type. The assigned ages for the plotting of the data are shown in parentheses and the abbreviations in the parentheses correspond to the alphabets in the diagram: Joubdo (J; 600 Ma), Adamsfield (Ad; 500 Ma), Ural (U; 400 Ma), Cariboo (Ca; 320 Ma), Atlin (At; 280 Ma), Tulameen (Tu; 205 Ma), Goodnews Bay (G; 215 Ma), Choco (Ch; 180 Ma), Kalimantan (K; 115 Ma), Sabah (S; 40 Ma), Teshio (Te; 110 Ma) and Onnabetsu (On; 120 Ma). Typical range of 2σ for each analysis is shown in a bar. Three solid lines show the bulk Earth evolution of the $^{187}Os/^{186}Os$ ratios: solid line with C1 is C1 chondritic evolution with 0.805 at 4.55 Ga [52] and 1.07 at present [53] with $^{187}Re/^{186}Os$ ratio of 3.70; solid line with C3O is C3O chondritic evolution which had the initial $^{187}Os/^{186}Os$ ratio of 0.805 at 4.55 Ga with the $^{187}Re/^{186}Os$ ratio of 3.32 [5]; solid line with M is bulk Earth evolution line proposed by Martin [1]. Depleted oceanic mantle evolution lines are broken lines. Long dash–short dash line: C1-like evolution until 2.0 Ga, then the decrease in the $^{187}Re/^{186}Os$ ratio by 40% by fractional fusion producing 1.98% melt. Short dash line: bulk Earth evolution proposed by Martin [1] until 2.0 Ga, then the decrease in the $^{187}Re/^{186}Os$ ratio by partial fusion producing 2% melt at 2.0 Ga.

osmium in Pt-Fe alloys from the Joubdo district have similar $^{187}Os/^{186}Os$ values (samples BM1928-247, 10, 12, 14; Table 1).

While the values of individual nuggets are similar in these ratios, there are significant variations in $^{187}Os/^{186}Os$ ratios among grains from one district (Fig. 3). The nuggets from the Atlin district, in which a dozen ultramafic bodies occur in an area of 35 km by 35 km, show $^{187}Os/^{186}Os$ ratios ranging from 1.00 to 1.09. Nuggets from Goodnews Bay also show a significant variation ranging from 1.03 to 1.12.

5. Discussion

5.1. Comparison with layered mafic intrusions

Large layered intrusions such as the Bushveld, Stillwater, and Freetown Complexes show wide variations in $^{187}Os/^{186}Os$ ratios (Fig. 2) [4,6,7,8,9]. The variations are attributed partly to intrusions of different magmas from different sources in the mantle [7], the assimilation of crustal rocks, and/or the incorporation of crustal Os by subsolidus hydrothermal activity [8].

The spread of $^{187}Os/^{186}Os$ ratios in the present samples is very limited compared with those for the large layered intrusions (Fig. 2). The observed small variation in $^{187}Os/^{186}Os$ ratios reflects several factors: the ensimatic environments of these intrusions, the Os-rich nature of the source, and the mode of their emplacement in the upper crustal level.

First, the layered intrusions were crystallized from tholeiitic magmas. Tholeiitic magmas contain much lower Os than ultramafic rocks [21], which makes $^{187}Os/^{186}Os$ ratios of tholeiitic magmas susceptible to change in the isotopic ratios.

Second, the magmas for the layered intrusions were emplaced in cratons, where the host rocks were geologically much older than the intrusions. The peridotites in the orogenic belts, on the other hand, were hosted in mafic igneous rocks and minor sedimentary rocks of similar ages. Due to much higher Os contents in peridotites than in the surrounding rocks and close $^{187}Os/^{186}Os$ ratios between the intrusions and the hosting country rocks, the interaction with the host rocks would not have seriously influenced the $^{187}Os/^{186}Os$ ratios of the ultramafic bodies.

Third, the relatively small sizes of peridotites were favourable for retaining the $^{187}Os/^{186}Os$ values of their sources because they did not have sufficient heat to assimilate nor to generate large magmatic-hydrothermal activity to incorporate crustal Os, as in the large layered intrusions.

Fourth, most of the peridotitic intrusions were emplaced in the upper crustal level as solid intrusions by obduction or diapiric processes. In particular, the syn-orogenic non-zoned-type ultramafic intrusions in ophiolite suites are believed to have been obducted to the upper crustal levels as "cold" intrusions. There was no opportunity for the solid intrusions to assimilate old host rocks nor to incorporate crustal Os during their crystallization in the mantle.

As described earlier, several ultramafic bodies are the cumulates of high-Mg boninitic magmas, which are the product of high degree partial melting of depleted mantle wedges above subduction zones. Because Os, Ir and Ru have lower solubility compared with Pt, Pd and Rh, the minerals of Os, Ir and Ru form in the very early stage of the crystallization of mafic magma [22], and occur in early crystallizing cumulate phases [23]. Therefore, the PGM would reflect the $^{187}Os/^{186}Os$ ratios of the source magma. In addition, the host volcanic rocks are similar in age and the assimilation would not have significantly altered the $^{187}Os/^{186}Os$ ratios of the magmas before the cumulate formation. The effect of assimilation is further evaluated in the following discussion.

5.2. Variation in $^{187}Os/^{186}Os$ ratios in one district

5.2.1. Variation due to sedimentary processes

Detailed mineralogical studies of PGM including exsolution textures of PGM and common occurrences of olivine and sulphides in the placer PGM grains have shown that PGM in placers were formed in ultramafic intrusions and that they were later mechanically eroded and transported to the site in placers [10,11,12,18]. Similar Os-isotope ratios of PGM in chromitites in ultramafic rocks and the associated placers in Borneo (laurites from chromitites in Pameli and Sungai Kalaan, and iridium grains in streams from Riam Kanan and Sungai Besar) and the Ural Mountains (U-45 from chromitites at Nizhni Tagil, and U-53 from the Omutnaya River; Table 1) confirm

this interpretation. No change in $^{187}Os/^{186}Os$ ratios took place during placer formation. The observed $^{187}Os/^{186}Os$ ratios of PGM from placers in this study, therefore, represent those of the responsible igneous rocks.

Although most PGM of alluvial placer origin occur along streams on ultramafic intrusions or immediately adjacent to the intrusions, some occur several km downstream from a series of ultramafic intrusions, such as the occurrences at Atlin, British Columbia. The variation of $^{187}Os/^{186}Os$ ratios may reflect the variation among intrusive bodies.

5.2.2. Isotopic variation during intrusion processes

The behaviour of PGE in magmas described in the preceding paragraphs suggests that Pt- and Pd-minerals formed later than Ru- and Os-minerals [22,23]. $^{187}Os/^{186}Os$ ratios of the Pd- and Pt- minerals may be modified due to contamination of crustal rocks. The observed values of $^{187}Os/^{186}Os$ ratios of PGM enclosed in Pt-Fe alloys are not different from those of Ir-Os alloys from one area, confirming that no appreciable change in $^{187}Os/^{186}Os$ ratios took place during the crystallization of the ultramafic magmas.

The small, but significant variations in $^{187}Os/^{186}Os$ ratios from one district are attributed to (1) the contribution of crustal Os by assimilation or circulating hydrothermal fluids, or (2) the heterogeneity in the source mantle. The former model implies that the minimum value in each area should represent the best value of the contemporaneous oceanic mantle source, because any crustal contribution would raise the $^{187}Os/^{186}Os$ ratios.

The contribution of crustal rocks is considered below.

Assimilation. The effect of the assimilation on $^{187}Os/^{186}Os$ ratios may be evaluated using the average concentration of Os in tholeiites, 0.02 ppb, and the average concentration of peridotites, 5 ppb [21]. The assimilation of tholeiites of equal weight which are 50 Ma older than the ultramafic rocks would raise $^{187}Os/^{186}Os$ ratios from 1.000 to 1.005. If the age of the host rocks is 100 Ma older than the ultramafic magma, and tholeiites of 50% of the weight of the magma are assimilated, the incorporation of host rocks would raise the $^{187}Os/^{186}Os$ ratio of the magma from

1.000 to 1.005. Much higher incorporation of host rocks is not geologically reasonable because it would change the chemistry of whole rocks.

If the ultramafic intrusion is composed of cumulates of boninitic magmas, we may expect that less amounts of assimilation are required to change the $^{187}Os/^{186}Os$ ratio of the magma. But, the MgO contents in boninites are high and similar to komatiites, suggesting a similar high degree of partial melting in the mantle and similar Os contents. The contents of Os in komatiites, 2 to 6 ppb [24,25], are compatible with those of peridotites [21]. Therefore, it is difficult to change $^{187}Os/^{186}Os$ ratios of boninites as ultramafic rocks.

The total spread in the $^{187}Os/^{186}Os$ ratios of Ir-Ru-Os grains is much larger than the variation expected from the assimilation, suggesting that the assimilation did not play a significant role in the observed variation in $^{187}Os/^{186}Os$ ratios. In addition, the occurrences of PGM in ultramafic intrusions suggest early formation during the crystallization history of magmas. The contents and relationships of PGE and MgO contents in komatiites also confirm that Ir, Ru, and Os precipitates early [25]. The evidence above suggests that Ir-Ru-Os minerals were most likely formed before significant assimilation of host rocks and that their isotopic signature will reflect those of the source mantle.

Hydrothermal activity. Two kinds of hydrothermal activity may be considered: the first occurring during intrusive activity and the latter during the serpentinization. As mentioned, the host volcanic rocks are similar in age and presumably have similar $^{187}Os/^{186}Os$ ratios. The contents of Os in the mafic volcanic rocks are an order of magnitude lower than those of ultramafic rocks. It is extremely difficult to raise $^{187}Os/^{186}Os$ ratios by the leaching of Os from mafic volcanic rocks during intrusive activity.

If hydrothermal activity involved a significant mobility of PGE, then pristine olivine and pyroxene chemistry in zoned-type indicates that the hydrothermal activity took place within the stability field of igneous minerals. It is difficult to discount this possibility, but it appears very unlikely based on the evidence below. Minerals and metals tend to precipitate from fluids where the changes of temperature and pressure occur. If an

intrusion-related hydrothermal process was involved for the formation of PGM, the most favourable sites for the mineralization would be the outer margins of intrusions, as found for Cu mineralization in porphyry-type deposits. Instead, PGM occur in the core of ultramafic intrusions.

The ultramafic bodies, especially the non-zoned-types, show varied degrees of serpentinization. The serpentinization is believed to have occurred during the obduction process of the ultramafic intrusions, which also obducted shallow marine sedimentary rocks and volcanic rocks. The sedimentary rocks may contain detritus derived from older terrains, and the incorporation of this old crustal Os would modify the ^{187}Os/^{186}Os ratios in the ultramafic rocks. But, comparison of the distribution of Ir, Pt and Pd between less serpentinized and completely serpentinized rocks suggests that the serpentinization has not resulted in significant mobilization of Os [26,27]. Platinum and Pd are considered to be more soluble compared with the rest of PGE [28]. Lack of enrichment or depletion of Pt and Pd in serpentinized rocks compared with less serpentinized counterparts precludes the possibility that significant amounts of Os were mobile from the surrounding host rocks during serpentinization.

The high mobility of Pt and Pd compared with Os and Ru in fluids suggests that Pt and Pd minerals may be high in serpentinized intrusions, if hydrothermal processes are significant for the formation of PGM. Contrary to the prediction, PGM in serpentinized non-zoned type intrusions are mostly Os and Ru minerals and the intrusions are low in Pt and Pd contents. Non-serpentinized zoned-type intrusions, on the other hand, commonly contain Pd and Pt minerals. Hydrothermal processes are therefore discounted as the significant cause for the variation in ^{187}Os/^{186}Os in each district.

5.3. Heterogeneity in the mantle.

We conclude that the variation in ^{187}Os/^{186}Os ratios (Fig. 3) is primarily due to the heterogeneity in the source upper oceanic mantle. It may be argued that the ultramafic sequence in ophiolites may represent juxtaposed slices of igneous bodies which were once separated in time and space. Peridotites of different origins may have been tectonically emplaced in one location: one formed in the ridge and one formed in supra-subduction zones. Some peridotites display evidence of several pulses of replenishing magma [23]. In any case, the sources of igneous rocks are oceanic mantle, and the spreading and obduction events for ophiolite formation took place in a geologically short time without significant transport of the plate [29]. Considering the long half life of ^{187}Re, the spread in ^{187}Os/^{186}Os ratios indicates their variation in the oceanic mantle.

The heterogeneity of ^{187}Os/^{186}Os ratios in the mantle in a given time suggests a long-lived heterogeneity in Re/Os ratios, over 1 b.y. It also implies that the calculation of Re/Os ratios and ^{187}Os/^{186}Os ratios of the bulk Earth needs the proper assessment of mass and isotopic ratios of different domains in the mantle.

5.3.1. The cause for low ^{187}Os/^{186}Os ratios compared with chondrite

As mentioned, the lowest value of the ^{187}Os/^{186}Os ratio in each district can safely be assumed to be the value of the mantle because no crustal processes would lower the values. All observed values, however, most likely represent those of the source mantle. The lowest values are generally lower than the C1 chondrite evolution curve (Fig. 3), suggesting that the mantle source area had a lower Re/Os ratio than C1 chondrite for a geologically long time (over 1 b.y.). The lowering of the Re/Os ratios may be attributed to primordially low Re/Os ratios of the mantle (model A) or the preferential extraction of Re from the mantle to the continental crustal reservoir by a prior partial melting process (model B). Model A means that the Earth's present mantle did not start with C1 chondritic Re/Os ratios, as proposed by Morgan [5].

Model A: low primordial Re/Os ratios in the mantle. High abundances of siderophile elements in the mantle compared to those expected from the core–mantle separation are commonly attributed to the incomplete partition of the elements during the separation or the addition of siderophile elements by accretion of chondrites after the core–mantle separation [30]. The ratios of refractory siderophile elements, which are similar to those of chondrites, and the high ratios of siderophile to chalcophile elements in the mantle

are favourable to multiple stages of accretion and core–mantle separation processes [31]. Morgan [5] proposed that the accreted chondrite in the mantle was mostly C3O type and the primordial value of the $^{187}Re/^{186}Os$ ratio of the mantle was 3.32. This is based on the assumption that the evolution of $^{187}Os/^{186}Os$ ratios in the mantle is homogeneous. The values of the evolution line of C3O chondrite are close to the observed values of the $^{187}Os/^{186}Os$ ratios. However, significant numbers of $^{187}Os/^{186}Os$ ratios are lower than the C3O evolution line (Fig. 3). In addition, the initial $^{187}Os/^{186}Os$ ratios of Archaean komatiites [24] are lower than the values expected from C3O evolution.

Re/Os weight ratios of chondrite vary from 0.05 to 0.12 ($^{187}Re/^{186}Os$ ratios from 2.1 to 5.0). C1 and C2 chondrites have relatively low Re/Os ratios compared with other chondrites, such as E-, H- and L-types [5]. If different types of chondrites were accreted to the Earth, the primordial Re/Os ratios would have been higher than those predicted from C1 and C2. Therefore, the model of the accretion of different types of chondrites is discounted as the major cause of the observed low $^{187}Os/^{186}Os$ ratios.

During the core–mantle separation, Re/Os may have increased in the silicate mantle. The partition coefficients of Re and Ir between liquid silicates to S-bearing metallic liquid [32] suggest that Re/Ir in liquid silicates is higher, and those among PGE suggest that Os has an even higher preference for sulphide melt [22]. The data suggest preferential removal of Os during the separation of S-bearing metal core and silicate mantle. Therefore, such a process could not have resulted in lower Re/Os ratios in the mantle. Primordially low Re/Os ratios which are due either to the bombardment of chondrite or core–mantle separation are, therefore, rejected as the explanation for the observed low $^{187}Os/^{186}Os$ ratios.

Model B: extraction of Re from mantle to continental crustal reservoir by partial melting as the cause for the low $^{187}Os/^{186}Os$. The weight ratios of Re/Os in basalts are over 30 [21,33]. These ratios are higher than those for the mantle-derived rocks, indicating that Re was preferentially partitioned into a melt during the partial melting in the mantle. After the partial melting, the resid-

ual mantle would be variably depleted in Re, and the $^{187}Os/^{186}Os$ ratio of the residue would not change as the rest of the mantle changed. Retention of the melts in the continental crust resulted in depletion of Re in the mantle. Positive ϵ_{Nd} and negative ϵ_{Sr} of mid-oceanic ridge basalts (MORB) and ultramafic bodies in ophiolites [34] are consistent with the interpretation that low $^{187}Os/^{186}Os$ ratios are due to the prior partial melting and the subsequent isolation from the rest of the mantle. The low $^{187}Os/^{186}Os$ ratios are also consistent with the observed chemistry of the ultramafic rocks, such as the depletion in light rare earth elements [34], low incompatible elements, and low and varied Re/Os ratios [35]. All of the isotope and trace element data suggest a long-lived heterogeneous oceanic mantle source region for these ultramafic intrusions.

The values of the $^{187}Os/^{186}Os$ ratios of the oceanic mantle may be modelled using the Re/Os ratios of the bulk Earth, the mean age of partial fusion, and the extent of partial melting. Because the data in this study show that the $^{187}Os/^{186}Os$ ratios of the present-day oceanic mantle are ~ 1.02, the extent of partial melting was calculated at a given age and the relationship between the mean age of partial fusion and the degree of the melting is illustrated in Fig 4. Two sets of calculations were made: one model assumes the evolution of $^{187}Os/^{186}Os$ ratios of the oceanic mantle from C1 chondritic bulk Earth [4], and the other assumes a higher bulk Earth value recently proposed by Martin [1].

The calculations used the experimentally determined distribution coefficient for Re between clinopyroxene and melt, 0.035, by Watson et al. [36]. The value is within the range of the empirical bulk distribution coefficient between the mantle and melt, 0.2 to 0.001, estimated from the contents of Re in basalts and komatiites by Walker et al. [3]. Clinopyroxene is most likely the main hosting silicate mineral for Re in the mantle since it incorporates far more incompatible elements than orthopyroxene and garnet. The distribution coefficient, 0.035 ± 0.005, should be the most warranted value between the bulk mantle and melt. The uncertainty of the value does not create significant changes in the results. For example, partial melting of 1.98 ± 0.30% is required at 2.0 Ga to obtain the present mantle value from
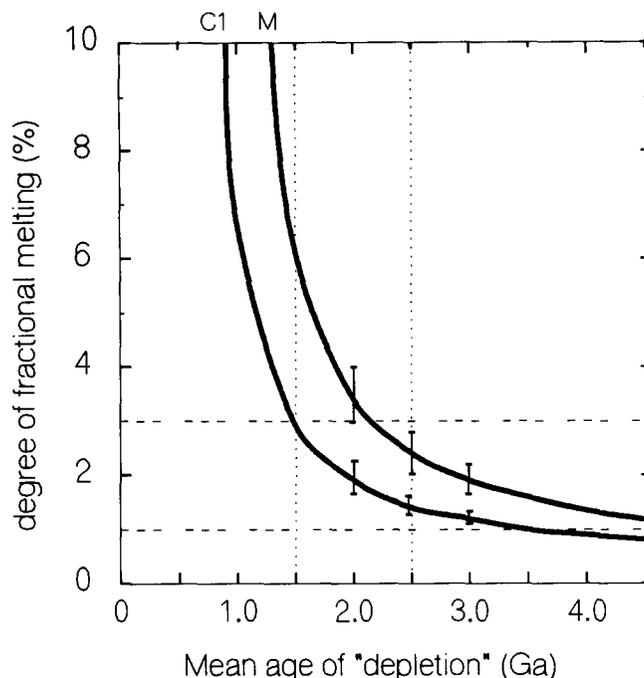
Fig. 4. Degree of melting and the mean age of the melting. Solid curves show the relationships between the degree of fractional melting and the age of the melting to attain $^{187}Os/^{186}Os$ ratio of 1.02 at present. The calculation used the distribution coefficient for Re and for Os 0.035 ± 0.005 and 120, respectively. The vertical bars are the ranges introduced by the uncertainty of the distribution coefficient for Re. Curve with C1 is the bulk Earth of C1 chondritic compositions. Curve with M is the bulk Earth of high Re/Os ratio, proposed by Martin [1]. Dotted lines show the probable mean ages of oceanic mantle [37]; dashed lines show the probable range of partial fusion [38,39].

the primitive mantle of C1 bulk Earth composition (Fig. 4).

The calculation used the bulk distribution coefficient for Os, 140, which is estimated from the contents of Os in basalts and komatiites [3]. A small difference in the distribution coefficient for Os does not affect the results of the calculations because the incompatibility of Re during the partial fusion primarily controls the depletion in Re/Os ratios in the residue.

Figure 4 illustrates that higher degree of partial melting is required if the mean age of depletion is younger and that higher bulk Earth Re/Os ratios [1] require higher degree of melting at a given age. If the bulk Earth has a high Re/Os ratio [1], the $^{187}Os/^{186}Os$ ratios of the bulk Earth would have attained 1.02 at 1.23 Ga. The mean age for the depletion must be older than the ages. If the mean age for the depletion is 1.5 Ga and 1.0 Ga, melting of 3.4% and 6.1 are required, respectively. If the bulk Earth has C1 chondritic composition, 6.8% and 1.98% of melt production

at 1.0 Ga and 2.0 Ga, respectively, is required to explain the observed values.

Because the ultramafic intrusions were derived from the oceanic mantle, the mantle sources for these intrusions may be approximated from MORB. Pb-isotopic arrays of the oceanic basalts suggest the mean age, 2.0 Ga [37]. Trace element studies [38] and other isotope systems [39] suggest that the mean degree of partial fusion is ~ 2%. These constraints support that the bulk Earth has a C1 chondritic Re/Os ratio. Depletion of Re/Os ratios in the mantle residue by production of 2% melt by fractional melting at ~ 2.0 Ga is consistent with the observed values [Fig. 3].

5.3.2. Variation in $^{187}Os/^{186}Os$ ratios in one district

The next question is the cause for the variation in $^{187}Os/^{186}Os$ ratios in one district. The variation appears to indicate long-lived heterogeneous distribution of Re and Os in the mantle. The variation may be due to "marble-cake" like local

heterogeneity in the mantle [2], and/or due to the heterogeneous distribution of S in the mantle.

Common occurrences of sulphides in mantle-derived rocks suggest that sulphides constitute common phases in the mantle [40,41]. Sulphide globules are also common in the quenched glass of MORB [42]. The negative pressure-dependence of S solubility in silicate melts [43] suggests that the source mantle for such basalts may be oversaturated in S, and that the sulphide phase existed at the source. The occurrences of sulphide inclusions in the primary minerals in harzburgite and lherzolite [44] support the view that a part of the depleted mantle contains sulphides. But other petrographic studies suggest that the partial melting may result in the almost total extraction of S from the residuum [22,45]. The evidence suggests heterogeneous distribution of sulphide in the mantle. Because both Re and Os are chalcophile, their behaviour is influenced by the distribution and amount of S in the mantle.

If S is oversaturated to silicate melt, Re/Os ratios of the source mantle may not change after the partial melting because there will not have been significant fractionation of the metals between the sulphide melt and silicate melts. The $^{187}Os/^{186}Os$ ratios of the mantle residues would change as those for the bulk Earth change. The observed low $^{187}Os/^{186}Os$ ratios suggest that S was not always in the residue during partial melting; S was impoverished. The common occurrence of S in the mantle rocks, therefore, requires the introduction of S from non-depleted sources or early separation of S from the melt while it was still in the mantle. Either mechanism would produce heterogeneity in Re/Os and subsequent variation in $^{187}Os/^{186}Os$ ratios.

The study of sulphides in mantle xenoliths shows that S may be present in the mantle as films on grain boundaries [46], or as CO_2-sulphide fluid [41,47]. Such S-bearing phases may be able to transport Re and Os from a more fertile source to the depleted mantle. Sulphides in the mantle may be concentrated in Re and Os, and thus act as a storage for Re and Os in the mantle.

The Re-Os isotopic system is similar to other isotopic systems, such as Rb-Sr and Sm-Nd. The radiogenic element is more incompatible during partial melting, and is stored in the continental crust. But, a non-lithophile Re-Os isotopic system may be decoupled from other radiogenic isotopic systems because of their chalcophile nature.

Our data of low $^{187}Os/^{186}Os$ ratios of the ultramafic rocks are generally compatible with the low and varied ratios of mantle xenoliths beneath southern Africa [3]. But, the values observed beneath southern Africa are as low as ~0.90, and they are generally lower than the values of the present results from the PGM in peridotite intrusions (Fig. 2). The discrepancy between the oceanic mantle and the sub-continental mantle beneath southern Africa may be attributed to (1) continental magmatism resulting in more efficient extraction of Re, (2) successive magma extraction from the same source area and isolation from the rest of the mantle, or (3) partial melting in the oceanic mantle more recent than the ~3.0 Ga for the southern African sub-continental mantle. The mean apparent age of the oceanic mantle, ~2.0 Ga [37], is not as old as that of the sub-continental mantle, but the latter option alone is not sufficient to explain the difference observed between the two mantles. Magmatism, such as kimberlite formation, would not have removed Re from the subcontinental lithosphere since kimberlites have rather low Re contents [48]. It appears that the models (1) and (3) may not satisfactorily explain the low Re/Os ratios in the sub-continental lithosphere. The remaining possibility is successive magma extraction and isolation. It is generally accepted that the cratonization and stabilization of the continents were accomplished through the devolatilization of the underlying mantle to form a refractory lithosphere [49]. The refractory parts have been physically separated in the mantle and it is likely that the physical nature of the refractory "keel" also allowed them to be chemically isolated from the rest of the mantle.

6. Conclusions

(1) PGM associated with ultramafic intrusions of various ages show a narrow spread in $^{187}Os/^{186}Os$ ratios from 0.992 to 1.121, much lower than those observed in large layered mafic intrusions. Because of the mode of the intrusions and their geological settings, these Os-isotope values are considered to be those of the source mantle.

(2) There is a significant variation in $^{187}Os/$$^{186}Os$ ratios in a given area. Because there was no change in $^{187}Os/^{186}Os$ ratios during placer formation and immobility of Os during serpentinization, the variation reflects the heterogeneity in $^{187}Os/^{186}Os$ ratios in the upper oceanic mantle due to a long-lived heterogeneity in Re/Os ratios (over 1 Ga).

The heterogeneity may be due to the local occurrences of ancient subducted components (marble-cake mantle; 1), and/or the occurrence of sulphides in the mantle.

(3) The lowest value from a given area is lower than the expected $^{187}Os/^{186}Os$ ratio for the evolution of C1 chondrite. The values are much lower than the ratio expected for a high Re/Os bulk Earth, proposed by Martin [1].

The low values cannot be attributed to primordially low Re/Os ratios of the mantle. The low values, therefore, are explained by the preferential extraction of Re into the continental crustal reservoir through partial melting processes. The data are consistent with the model in which the oceanic mantle had the initial C1 chondritic Re/Os ratios until 2.0 Ga, and underwent ~ 2% fractional partial melting to reduce Re/Os ratios by 40%. If the bulk Earth has higher Re/Os ratios, as proposed by Martin [1], then it requires larger amounts of partial melting or older mean age of the fusion, ~ 3.0 Ga. The former model is preferred because the mean age and the degree of partial fusion are in general agreement with other isotopic and trace element studies [38,39].

(4) The variation in $^{187}Os/^{186}Os$ ratios in one area is attributed to local-scale heterogeneity in the mantle [2], and/or the presence of S in the mantle.

Rhenium, which would be extracted from the source during partial melting, would be separated into S-melt while the silicate melt was still in the mantle. Infiltrating sulphide and CO_2-sulphide melt in the mantle may transport Re and Os from a more fertile region into the depleted mantle source. Common occurrences of sulphides in mantle minerals and along grain boundaries of xenoliths appear to support this model.

Much lower $^{187}Os/^{186}Os$ ratios observed in the sub-continental mantle by Walker et al. [3] may suggest that the oceanic mantle was not so isolated from the rest of the mantle.

Appendix—description of studied areas

Non-zoned-types

Adamsfield, Tasmania. The Adamsfield Ultramafic Complex (AUC) is one of a dozen Tasmanian ultramafic–mafic complexes in the ophiolite sequence of Cambrian age in the Tasman Geosyncline. The AUC, which is composed of dunite and olivine orthopyroxenite, was originally emplaced in the Cambrian sedimentary rocks of the Adamsfield Troughs and re-intruded into the overlying Ordovician sedimentary rocks, forming the core of a large anticline [19]. The ultramafic rocks are low in TiO_2 and are believed to have formed in an immature arc above the subduction zone [13]. Alluvial PGM, mostly iridian osmium with minor rutheniridosmine, are found along streams as well as in the Ordovician sedimentary rocks overlying the AUC. Olivine and pyroxene inclusions in the alluvial PGM are similar in composition to those in the AUC, confirming the derivation from dunite.

Atlin district, British Columbia. The area is located in northwestern British Columbia near the Yukon border. The Atlin intrusions consist of a dozen small ultramafic intrusions associated with the ophiolite sequence of the Pennsylvanian/Permian Cache Creek Group [56]. They are composed of peridotite and most are massive except for the Mt. O'Keefe intrusion, which shows crude layering of dunite [56]. The ultramafic intrusions are cut by the late Cretaceous Coast Range granites.

Bullion mine, Cariboo Mining District, British Columbia. The Bullion mine is located ~ 4 miles west of the outlet of Quesnel Lake in southwestern British Columbia. The source of PGM is serpentine belts in the Carboniferous Slide Mountain Terrane. The terrane is composed of ultramafic igneous rocks and mafic volcanic rocks, and attaches to the western

margin of the Barkerville Terrane of late Precambrian to Paleozoic volcano-sedimentary rocks [57].

Goodnews Bay, Alaska. PGM grains, mainly Pt-Fe alloys, iridium, and sperrylite, occur along the streams east of the Goodnews Bay Ultramafic Complex, along the sea shore, and in the past-foreland west of the complex. The Ultramafic Complex, ~ 2 km by 5 km, is concentrically zoned and forms a topographically high point, Red Mountain. The Jurassic Complex intruded in the NE trending late Triassic to early Jurassic volcanic and sedimentary belt [58]. The Mesozoic terrane accreted to a Paleozoic volcano-sedimentary terrane to the north. The ultramafic rocks are partially serpentinized, but primary olivine and pyroxene are well preserved.

Sabah, Malaysia. The Darvel Bay–Labuk–Palawan Ophiolite Complex occurs in the northcentral part of Borneo Island and swings east to Darvel Bay at the eastern end of the island. The ophiolite complex extends north on Palawan Island in the Philippines. The ultramafic suite consists of harzburgite, pyroxenite, and serpentinized dunite. The Ar-age of metamorphic minerals on Palawan Island, 36 Ma, and the host rock stratigraphy of Borneo Island indicate a Miocene age for the complex [59].

Kalimantan, Indonesia. Two dismembered ultramafic bodies occur in the southern part of Kalimantan, the Meratus and Bobaris Mountain Ranges. They are composed of dunite, lherzolite, harzburgite, olivine clinopyroxenite, and are believed to represent the uppermost part of the oceanic mantle [55]. PGE-bearing chromitites are surrounded by dunite and then by harzburgite [55]. The rocks were obducted during the subduction of the Sundaland Plate, ~ 114 Ma, following rifting of the Paleo-Sulawesi Sea [55]. PGM in the alluvial placers, developed in the ophiolitic assemblage, are Pt-Fe alloy, osmium, iridian osmium, iridium, laurite, and Pd-As minerals [55,60].

Teshio and Onnabetsu, Central Hokkaido Island, Japan. Two north-trending ultramafic belts run parallel to one another in the central part of Hokkaido Island: the Kamuikotan tectonic belt to the west and the Hidaka serpentinite belt to the east. The Teshio and Onnabetsu deposits are at the northern end of the Kamuikotan belt, where four similar ultramafic bodies, which consist of dunite and harzburgite, intruded into the early Cretaceous Sorachi Group volcano-sedimentary rocks: the Horokanai, Inushibetsu, Takadomari, and Takasu intrusions. The ultramafic rocks belong to low Al and Ti-type ultramafic bodies (< 0.05 wt.% TiO_2 and < ~ 2% Al_2O_3 [19]).

Zoned-types

Joubdo, western Ethiopia. The Joubdo (Yubdo) district is within the Mozambique mobile belt, a late Proterozoic orogenic belt in eastern Africa. Several ultramafic bodies, including the Daletti, Tulu Dimtu, and Joubdo Complexes, form a NNE-trending belt along the boundary between a high-grade felsic gneiss to the east and a greenschist facies volcano-sedimentary terrane to the west, which was accreted during the late Proterozoic subduction [61]. The precise U-Pb zircon ages of granitoids from the area constrain the age of the ultramafic

complexes, 635 to 570 Ma [61]. The age is in accordance with the end of thermal activity in the area, ~ 600 Ma, based on K-Ar data [62].

The intrusive body is a typical Alaskan-type with a massive dunite core surrounded by minor wehrlite, then pyroxenite, and by gabbros. Most grains of PGM were recovered from the capping eluvium on the central dunite body [63]. Lesser amounts occur along the Birbir River whose tributaries cut the ultramafic complex.

Ural Mountains. Two types of ultramafic intrusive belts are known in the area: one belt with ophiolitic non-zoned-type intrusions and another ~ 80 km to the west consisting of zoned ultramafic bodies. One sample came from the Nizhni Tagil dunite massif in the core of a dunite–clinopyroxenite–gabbro complex, which is hosted by the pillowed lavas and related intrusions of the late Silurian and mafic to intermediate calc-alkaline rocks of early Devonian time. The diapiric emplacement of the ultramafic complexes in the area is believed to be related to the early Devonian igneous activity [64].

PGM are concentrated within chromitites within dunite massifs, and more than 600 sites of the occurrences of PGM are recorded in the area [64]. In some complexes, wehrlite and plagioclase pyroxenite layers are found between the dunite and pyroxenite. The outermost part may be quartz diorite and syenite. The dunite is generally free from serpentinization, and primary olivine and pyroxene crystals are well preserved [65]. The lithology of the host rocks, the occurrence of PGM, and the mineralogy are similar to those in the Tulameen Complex in B.C.

Tulameen, British Columbia. The Tulameen Ultramafic Complex, ~ 6 km by ~ 20 km, is located within the southwestern Intermontane Belt, immediately east of the junction of the Quesnelklia tectono-stratigraphic terrane and the Mount Lytton Plutonic Complex. The intrusive suite was emplaced into the metasedimentary and intermediate to felsic metavolcanic rocks of the Upper Triassic Nicola Group. The Tulameen Complex consists of a core of chromitiferous dunite, olivine clinopyroxenite, hornblende clinopyroxenite, and gabbroic rocks [12,14]. Pyroxene syenite, which is believed to have been emplaced at the same time as the ultramafic intrusions, occurs adjacent to the ultramafic complex. The ultramafic intrusion is syn- to late-tectonic, and the whole suite has undergone ductile and brittle deformation.

The U-Pb zircon ages of the syenitic phase give the date of 209 Ma and $(^{87}Sr/^{86}Sr)_{initial}$ ratios of 0.7030 to 0.7046 (J. Rublee, written commun., 1989). PGE in the complex are concentrated in the chromitites in the dunite cores, and the comparison of PGM from placers and chromitites shows the derivation of placer PGM from the dunite source [12]. Studied samples come from Granite Creek and Bear Creek, also called Lawless Creek. Both run directly west of the Tulameen Complex.

Choco, western Colombia. Because of the poor understanding of the geology of this area, located in the Cordillera Occidental, it is difficult to estimate the nature of the ultramafic intrusions at the source. But, the occurrences of PGM in the serpentinized dunite and pyroxenite, west of Cerro Irro, and the occurrence of dunite, pyroxenite, and gabbro boulders together with PGM along the streams in the area suggest

that the source igneous rocks are Alaskan-type ultramafic intrusions [66].

References

1 C.E. Martin, Osmium isotopic characteristics of mantle-derived rocks, Geochim. Cosmochim. Acta 55, 1421–1434, 1991.

2 C.J. Allègre and D.L. Turcotte, Implications of a two-component marble-cake mantle, Nature 323, 123–127, 1986.

3 R.J. Walker, R.W. Carlson, S.B. Shirey and F.R. Boyd, Os, Sr, Nd and Pb isotope systematics of southern African peridotite xenoliths; implications for the chemical evolution of subcontinental mantle, Geochim. Cosmochim. Acta 53, 1583–1595, 1989.

4 C.J. Allègre and J.M. Luck, Osmium isotopes as petrogenetic and geological tracers, Earth Planet. Sci. Lett. 48, 148–154, 1980.

5 J.W. Morgan, Osmium isotope constraints on Earth's late accretionary history, Nature 317, 703–705, 1985.

6 C.E. Martin, Re-Os isotopic investigation of the Stillwater Complex, Montana, Earth Planet. Sci. Lett. 93, 336–344, 1989.

7 D.D. Lambert, J.W. Morgan, R.J. Walker, S.B. Shirey, R.W. Carlson, M.L. Zientek and M.S. Koski, Rhenium–osmium and samarium–neodymium isotopic systematics of the Stillwater complex, Science 244, 1169–1174, 1989.

8 S.R. Hart and E.D. Kinloch, Osmium isotope systematics in Witwatersrand and Bushveld ore deposits, Econ. Geol. 84, 1651–1655, 1989.

9 K. Hattori, L.J. Cabri and S.R. Hart, Os-isotope ratios of platinum group mineral nugget associated with Freetown Layered Intrusive Complex, Sierra Leone, Contrib. Mineral. Petrol., in press, 1991.

10 R.J. Ford, Platinum-group minerals in Tasmania, Econ. Geol. 76, 498–504, 1981.

11 D. Hagen, Th. Weiser and T. Htay, Platinum-group minerals in Quaternary gold placers in the upper Chindwin area of Northern Burma, Mineral. Petrol. 42, 265–286, 1990.

12 G.T. Nixon, L.J. Cabri and J.H.G. Laflamme, Platinum-group element mineralization in lode and placer deposits associated with the Tulameen Alaskan-type complex, British Columbia, Can. Mineral. 28, 503–535, 1990.

13 G. Serri, The petrochemistry of ophiolite gabbroic complexes: a key for the classification of ophiolites into low-Ti and high-Ti types, Earth Planet. Sci. Lett. 52, 203–212, 1981.

14 D.C. Findlay, Origin of the Tulameen ultramafic–gabbro complex, southern British Columbia, Can. J. Earth Sci. 6, 399, 1969.

15 W.K. Conrad and R.W. Kay, Ultramafic and mafic inclusions from Adak island crystallization history and implications for the nature of primary magmas and crustal evolution in the Aleutian island arc, J. Petrol. 25, 88–125, 1984.

16 P.B. Kelemen and M.S. Ghiorso, Assimilation of peridotite in zoned calc-alkaline plutonic complexes; evidence from the Big Jim complex, Washington, Cascades, Contrib. Mineral. Petrol. 94, 12–28, 1986.

17 D.C. Harris and L.J. Cabri, Nomenclature of platinum-group-element alloys: review and revision, Can. Mineral. 29, 231–238, 1991.

18 L.J. Cabri and D.C. Harris, Zoning in Os-Ir alloys and the relation of the geological and tectonic environment of the source rocks to the bulk Pt; Pt + Ir + Os for placers, Can. Mineral. 13, 266–274, 1975.

19 R. Varne and A.V. Brown, The geology and petrology of the Adamsfieled ultramafic complex, Tasmania, Contrib. Mineral. Petrol. 67, 195–207, 1978.

20 T. Katoh and M. Nakagawa, Tectogenesis of ultramafic rocks in the Kamuikotan tectonic belt, Hokkaido, Japan, Monograph Assoc. Geol. Collab. Jpn. 31, 119–135, 1986.

21 C.-L. Chou, D.M. Shaw and J.H. Crocket, Siderophile trace elements in the Earth's oceanic crust and upper mantle, J. Geophys. Res. 88, A507–518, 1983.

22 S.J. Barnes, A.J. Naldrett and M.P. Gorton, The origin of the fractionation of PGE in terrestrial magma, Chem. Geol. 53, 303–323, 1985.

23 D.C. Peck and R.R. Keays, Geology, geochemistry and origin of platinum-group element chromitite occurrences in the Heazlewood River complex, Tasmania, Econ. Geol. 85, 765–793, 1990.

24 R.J. Walker, S.B. Shirey and O. Stecher, Comparative Re-Os, Sm-Nd and Rb-Sr isotope and trace element systematics for Archaean komatiite flows from Munro Township, Abitibi belt, Ontario, Earth Planet. Sci. Lett. 87, 1–12, 1988.

25 G.E. Brugmann, N.T. Arndt, A.W. Hofmann and H.J. Tobschall, Precious element abundances in komatiites suites from Alexo, Ontario and Gorgona Island, Colombia, Geochim. Cosmochim. Acta 51, 2159–2169, 1987.

26 J.R. Ross and R.R. Keays, Precious metals in volcanic-type nickel sulfide deposits in Western Australia, I. Relationship with the composition of the ores and their host rocks, Can. Mineral. 17, 417–435, 1979.

27 I.O. Oshin and H.J. Crocket, Noble metals in Thetford Mines ophiolites, Quebec, Canada, I. Distribution of gold, iridium, platinum, and palladium in the ultramafic and gabbroic rocks, Econ. Geol., 77, 1556–1570, 1982.

28 B.W. Mountain and S.A. Wood, Chemical controls on the solubility, transport and deposition of platinum and palladium in hydrothermal solutions: a thermodynamic approach, Econ. Geol. 83, 492–510, 1988.

29 J.F. Casey and J.F. Dewy, Initiation of subduction zones along transform and accreting plate boundaries, triple-junction evolution, and forearc spreading centres—implications for ophiolitic geology and obduction, in: Ophiolites and Oceanic Lithosphere, I.G. Gass, S.J. Lippard and A.W. Shelton, eds., pp. 269–290, Geol. Soc. London Spec. Publ. 13, 1984.

30 S.S. Sun, Multistage accretion and core formation of the Earth, Nature 313, 628–629, 1985.

31 H.F. Newsom and H. Palme, The depletion of siderophile elements in the Earth's mantle: new evidence from molybdenum and tungsten, Earth Planet. Sci. Lett. 69, 354–364, 1984.

32 J.H. Jones and M.J. Drake, Geochemical constraints on core formation in the Earth, Nature, 322, 221–228.

33 J. Hertogen, M-J. Jassens and H. Palme, Trace elements in ocean ridge basalt glasses: implications for fractiona-

tions during mantle evolution and petrogenesis, Geochim. Cosmochim. Acta 44, 2125–2143, 1980.

34 M.A. Menzies, Chemical and isotopic heterogeneity in orogenic and ophiolitic peridotites, in: Ophiolites and Oceanic Lithosphere, I.G. Gass, S.J. Lippard and A.W. Shelton, eds, pp. 231–240, Geol. Soc. London Spec. Publ. 13, 1984.

35 W.F. McDonough, Chemical and isotopic systematics of continental mantle, EOS Trans. Am. Geophys. Union 71, 1670, 1990.

36 E.B. Watson, D.B. Othman, J-M. Luck and A.W.Hofmann, Partitioning of U, Pb, Cs, Yb, Hf, Re and Os between chromian diopsidic pyroxene and haplobasaltic liquid, Chem. Geol. 62, 191–208, 1987.

37 S.R. Hart, Large scale isotope anomaly in the southern hemisphere mantle, Nature 309, 753–757, 1984.

38 A.W. Hofmann, Chemical differentiation of the Earth: the relationship between mantle, continental crust and oceanic crust, Earth Planet. Sci. Lett. 90, 297–314, 1988.

39 V.J.M. Salters and S.R. Hart, The mantle sources of ocean ridges, islands and arcs: the Hf-isotope connection, Earth Planet. Sci. Lett. 104, 364–380, 1991.

40 R. Peterson and D. Francis, The origin of sulfide inclusions in pyroxene megacrysts, Am. Mineral. 62 1049–1051, 1977.

41 T. Andersen, W.L. Griffin and S. O'Reilly, Primary sulphide melt inclusions in mantle-derived megacrysts and pyroxenites, Lithos 20, 279–294, 1987.

42 E.A. Mathez, Sulfur solubility and magmatic sulfides in submarine basalt glass, J. Geophys. Res. 81, 4269–4276, 1976.

43 R.F. Wendlandt, Sulfide saturation of basalts and andesite melts at high pressures and temperatures, Am. Mineral. 67, 877–885, 1982.

44 J.P. Lorand, Cu-Fe-Ni-S mineral assemblages in upper-mantle peridotites from the Table Mountain and Blow-Me-Down Mountain ophiolite massifs (Bay of Islands area, Newfoundland): their relationships with fluids and silicate melts, Lithos 20, 59–76, 1987.

45 S.J. Edwards, Harzburgites and refractory melts in the Lewis Hills massif, Bay of Islands ophiolite complex: the base-metals and precious metals story, Can. Mineral. 28, 537–552, 1990.

46 R.H. Mitchell and R.R. Keays, Abundance and distribution of gold, palladium and iridium in some spinel and garnet lherzolites: implications for the nature and origin of precious metal-rich intergranular components in the upper mantle, Geochim. Cosmochim. Acta 45, 2425–2442, 1981.

47 V.I. Kovalenko, I.P. Solovova, V.B. Naumov, I.D. Ryabchikov, D.A. Ionov and A.I. Isepin, Mantle mineral formation with the participation of a CO_2-sulfide-silicate fluid, Geochim. Int. 7, 66–79, 1986.

48 J.W. Morgan and J.F. Lovering, Rhenium and osmium abundances in some igneous and metamorphic rocks, Earth Planet. Sci. Lett. 3, 219–224, 1967.

49 H.N. Pollack, Cratonization and thermal evolution of the mantle, Earth Planet. Sci. Lett. 80, 175–182, 1986.

50 R.J. Walker, L.M. Echerverria, S.B. Shirey and M.F. Horan, Re-Os isotopic constraints on the origin of volcanic rocks, Gorgona Island, Columbia: Os isotopic evidence for ancient heterogeneities in the mantle, Contrib. Mineral. Petrol. 107, 150–162, 1991.

51 M.R. Pegrem, J.M. Luck and C.J. Allègre, Osmium isotopic compositions from basalts (abstr.), Chem. Geol. 70, 55, 1988.

52 J.M.Luck and C.J. Allègre, ^{187}Re-^{186}Os systematics in meteorites and cosmochemical consequences, Nature 302, 130–132.

53 R.J. Walker and J.W. Morgan, Rhenium-osmium isotope systematics of carbonaceous chondrites, Science 243, 519–522, 1989.

54 D.C. Harris and L.J. Cabri, The nomenclature of the natural alloys of osmium–iridium and ruthenium based on new compositional data of alloys from world-wide occurrences, Can. Mineral. 12, 104–112, 1973.

55 K.-P. Burgath, Platinum-group minerals in ophiolitic chromitites and alluvial placer deposits, Meratus–Bobaris area, southeast Kalimantan, in: Geo-Platinum 87, H.M. Prichard, P.J. Potts, J.F.W. Bowles and S.J. Cribb, eds., pp. 383–403, Elsevier Applied Sci., London, 1988.

56 J.D. Atken, Atlin Map-Area, British Columbia, Geol. Surv. Can. Mem. 307, 89 pp., 1959.

57 L.C. Struik, Structural Geology of the Cariboo Gold Mining District, East-central British Columbia, Geol. Surv. Can. Mem. 421, 100 pp., 1988.

58 J.C. Barker and K. Lamal, Offshore extension of platiniferous bedrock and associated sedimentation of the Goodnews Bay ultramafic complex, Alaska, Mar. Min. 8, 365–390, 1989.

59 C. Hutchison, Ophiolite in southeast Asia, Bull. Geol. Soc. Am. 86, 797–806, 1975.

60 E.F. Stumpfl and A.M. Clark, Electron-probe microanalysis of gold platinoid concentrates from southeast Borneo, Trans. Inst. Min. Metall. 74, 933–946, 1966.

61 T. Ayalew, K. Bell, J.M. Moore and R.R. Parrish, U-Pb and Rb-Sr geochronology of the Western Ethiopian Shield, Geol. Soc. Am. Bull. 102, 1309–1316, 1990.

62 A.S. Rogers, J.A. Miller and P.A. Mohr, Age determinations on some Ethiopian basement rocks, Nature 206, 1021–1023, 1965.

63 J. Ottermann and S.S. Augustithis, Geochemistry and origin of platinum-nuggets in lateritic covers from ultrabasic rocks and Birbirites of W. Ethiopia, Mineral. Deposita 1, 269–277, 1967.

64 L.J. Cabri and A.D. Genkin, Re-examination of Pt-alloys from lode and placer deposits, Ural, Can. Mineral. 29, 3, in press.

65 A.G. Betechtin, Mikroskopische Untersuchungen an Platinerzen aus dem Ural, Neues Jahrb. Mineral. Abh. 97, 1–34, 1961.

66 J.J. O'Neil and H.C. Gunning, Platinum and allied metal deposits of Canada, Can. Geol. Surv. Econ. Geol. 13, 165 pp.